Comparative Study of Single-Wood Biomass Model at Plot Level Based on Multi-Source LiDAR

Ying Zhang [1,†], Siyu Xue [2,3,†], Shengqiu Liu [4], Xianliang Li [4], Qijun Fan [4], Nina Xiong [2,3] and Jia Wang [2,3,*]

1   School of Economics and Management, Beijing Forestry University, No. 35, Qinghua East Road, Haidian District, Beijing 100083, China
2   Beijing Key Laboratory of Precision Forestry, Beijing Forestry University, No. 35, Qinghua East Road, Haidian District, Beijing 100083, China
3   School of Forestry, Beijing Forestry University, No. 35, Qinghua East Road, Haidian District, Beijing 100083, China
4   Guangxi Key Laboratory of Germplasm Innovation and Utilization of Specialty Commercial Crops in North Guangxi, Guangxi Academy of Specialty Crops, Guilin 541004, China
*   Correspondence: wangjia2009@bjfu.edu.cn
†   These authors contributed equally to this work.

Abstract: Forests play an important role in promoting carbon cycling and mitigating the urban heat island effect as one of the world's major carbon storages. Scientifically quantifying tree biomass is the basis for assessing tree carbon storage and other ecosystem functions. In this study, a sample plot of *Populus tomentosa* plantation in the Olympic Forest Park in Beijing was selected as the research object. Point cloud data from three types of laser scanners, including terrestrial laser scanner (TLS), backpack laser scanner (BLS), and handheld laser scanner (HLS), were used to estimate the biomass of single tree trunks, branches, leaves, and aboveground total biomass based on the Allometric Biomass Model (ABM) and Advanced Quantitative Structure Model (AdQSM). The following conclusions were drawn from the estimation results: (1) For the three types of laser scanner point clouds, the biomass estimation values obtained using the AdQSM model were generally higher than those obtained using the Allometric Biomass Model. However, the estimation values obtained using the two models were similar, especially for tree trunks and total biomass. (2) For total biomass and individual biomass components of single trees, the results obtained from handheld and terrestrial laser scanner point clouds are consistent; however, they show some differences from the results obtained from backpack-mounted point clouds. This study further enriches the methodological system for estimating forest biomass, providing a theoretical basis and reference for more accurate estimates of forest biomass and more sustainable forest management.

Keywords: allometric biomass model; advanced quantitative structure model (AdQSM); terrestrial laser scanner (TLS); backpack laser scan (BLS); handheld laser scan (HLS)

1. Introduction

With the rapid development of urbanization in China, environmental issues such as excessive CO_2 emissions, climate warming, and worsening air pollution have become increasingly prominent. The role of urban trees has become more and more important. Urban trees can alleviate the urban heat island effect, regulate local climate, and provide recognized ecosystem services [1]. They absorb a large amount of carbon from the atmosphere through photosynthesis and store it in plant tissues, becoming an important carbon storage. Forests are an important component of global terrestrial ecosystems and store over 80% of carbon [2]. They have various ecological functions, including carbon sequestration, oxygen release, water conservation, climate regulation, biodiversity protection, and maintaining global carbon balance [3–5]. The carbon sequestration function of forests has been established, and the methods for measuring and evaluating their ability to sequester

atmospheric CO_2 have also received increasing attention. A study by Price et al. [6] showed that 9.4 million tons of carbon are stored in trees in Swiss residential areas. However, since the spatial area of urban trees occupies a relatively small proportion of global forest cover and their contribution to the global carbon cycle is relatively dispersed, related research is seldom considered. Nevertheless, research on monitoring and assessing the carbon storage of urban trees and evaluating methods for doing so is of great significance for fully realizing their ecosystem functions. [7,8].

Measuring aboveground biomass (AGB) is a reliable approach for assessing tree carbon storage and other ecosystem functions, gaining increasing attention in forestry surveys. Davies [9] showed that trees account for 97% of urban AGB, making accurate estimations of tree biomass crucial not only for forestation planning, forest resource monitoring, and evaluation of forest ecological values but also for directly impacting policy-making in forest timber harvesting, protection, and management. The assessment of forest biomass includes both aboveground and belowground biomass. However, due to the difficulty in quantifying belowground biomass and its relatively smaller proportion compared to aboveground biomass [10], research on forest biomass primarily focuses on aboveground biomass. Hereafter, unless specifically stated, biomass refers to aboveground biomass in this article. Current methods for estimating biomass include the felling method, allometric biomass models, and quantitative structure models. The felling method involves cutting down all sample trees (trees, shrubs, etc.) within a plot, and then drying and weighing their parts to determine their biomass, which not only destroys the forest structure but also consumes significant time, labor, resources, and financial investment. Allometric biomass models and quantitative structure models allow for non-destructive estimation of forest biomass, avoiding the extensive resource consumption of traditional sampling surveys and improving the timeliness and spatial completeness of data [9], which is of significant importance in advancing forestry survey techniques. However, current comparative studies on these two models are still limited.

For forest data collection, LiDAR technology has clear advantages over traditional optical remote sensing [11–13]. It uses lasers as the light source, scanning and ranging to quickly acquire high-precision three-dimensional point clouds, thereby obtaining the three-dimensional structure of forest stands. This technique has achieved certain accomplishments in the quantitative measurement and inversion of forest parameters [14–16]. Ground-based LiDAR is often used for collecting detailed three-dimensional data on single targets or on a small scale, capable of obtaining accurate under-canopy vegetation three-dimensional information. Based on its operating modes, it can be divided into Terrestrial Laser Scanner (TLS), Backpack Laser Scanner (BLS), and Handheld Laser Scanner (HLS) [17]. TLS replaces traditional felling measurements, allowing for the automatic acquisition of detailed and accurate internal forest three-dimensional information without damaging the forests, and accurately extracting individual tree structure parameters [18,19]. In comparison, Mobile Laser Scanner (MLS) integrates the Global Navigation Satellite System and Inertial Measurement Units, making real-time scanning and mapping possible without the need for target setting, stationing, scanning, and moving as required by TLS, thus improving the efficiency of forest resource surveys [20]. As a form of MLS, Backpack Laser Scanner (BLS) integrates real-time positioning and mapping to build SLAM technology, is convenient to carry and operate, and effectively addresses the constraints of weather, terrain, and satellite navigation [21,22]. As another variant of MLS, Handheld Laser Scanner (HLS) uses a human platform to obtain real-time point cloud data, employing high-precision real-time positioning and mapping algorithms for data stitching, overcoming the weak satellite signal issue under forest canopies with its flexible scanning method and higher efficiency [23]. Yao et al. [24], Raumonen et al. [25], Zheng Yujie et al. [26], Wang Chuhong et al. [27], and Fan Weiwei et al. [28] have conducted certain research and applications in estimating individual tree biomass using stationary ground-based LiDAR technology, and handheld mobile LiDAR technology, but the application of backpack LiDAR technology in biomass assessment is still less common.

The allometric biomass equation model method for biomass measurement is a current approach based on non-destructive field measurements of tree structural parameters such as Diameter at Breast Height (DBH) and tree height (H), followed by the development of allometric biomass equation models [29,30]. Bi et al. [31] obtained accurate structural parameters of trees and applied species-specific allometric biomass models to calculate the biomass of forest stands, demonstrating the accuracy and effectiveness of using non-destructive forest biomass measurements. Seidel et al. [32] measured individual tree DBHs from TLS data and predicted the trees' biomass using regional allometric biomass models, achieving an average relative error of only 16.4%. This represented a significant reduction in fieldwork in dense forests compared to traditional manual measurement methods. Nonetheless, fundamentally, this non-destructive biomass estimation approach is still based on limited structural parameters and relies on empirical relationships derived from allometric biomass models. It still involves significant uncertainty in estimating the biomass of trees with complex structures.

Consequently, Raumonen et al. [25] developed a Quantitative Structure Model (QSM) algorithm for reconstructing the complete morphological structure of individual trees from TLS point cloud data. This method employs least squares and cylindrical fitting algorithms to directly calculate the volume of trees (including trunks and branches) from the reconstructed 3D structural model. The volume of the tree, multiplied by the basic wood density value of the corresponding tree species, can be converted into the tree's biomass. This approach estimates tree biomass based on a realistic morphological structure model of a specific tree species, fundamentally differing from allometric biomass models that rely solely on limited forest parameter factors.

Two mainstream implementations of the QSM algorithm have significantly contributed to this field of research. The first, developed by Calders et al. [33], known as TreeQSM, reconstructs the woody structure of trees from point cloud data. It employs cylindrical fitting to map the tree's topological structure and calculates the volume of each cylinder to estimate the biomass of both trunks and branches. Comparisons with biomass obtained through destructive sampling indicated that the biomass estimations for species like oak and eucalyptus using TreeQSM were higher by 15.3% to 18.8% and had a relative root mean square error (rRMSE) for eucalyptus of about 28.5%, showcasing high estimation precision. The second notable QSM implementation is the SimpleTree algorithm, proposed by Hackenberg et al. [34]. This method divides the tree point cloud into two sections (upper and lower) for separate processing, with the upper section comprising the trunk and branches and the lower section comprising the stump. Cylindrical fitting is then used to connect these two sections into a cohesive cylindrical tree model based on ground-based laser scanning data. The SimpleTree approach demonstrated high accuracy, with the lowest biomass correlation coefficient in their dataset samples being 0.92. Building upon these methods, Fan et al. [35] introduced the Advanced Quantitative Structure Model (AdQSM) to address the scarcity of comprehensive QSM methods. AdQSM focuses on the automatic reconstruction of the fine geometric structures of individual tree limbs from various types of LiDAR point cloud data, addressing the lack of generality and robustness in conventional tree modeling studies. By examining the reconstruction accuracy and effectiveness across different LiDAR data types, geographic regions, and tree shapes and sizes, the AdQSM method achieved consistency correlation coefficients (CCC) and determination coefficients (R2) of 0.98 and 0.95, respectively, outperforming mainstream methods by 1% to 4% in precision. Additionally, AdQSM enables the automatic, batch extraction of highly accurate structural parameters such as DBH and tree height, offering a cost-effective solution for tree structure reconstruction and parameter extraction.

This study, utilizing terrestrial, backpack, and handheld LiDAR point cloud data at plot level for individual tree segmentation, employed both the allometric biomass model and the Advanced Quantitative Structure Model (AdQSM) for estimating the biomass of individual trees. The results are compared and analyzed to further verify the applicability of these two theoretical models, enrich the methodological system for estimating forest biomass,

and provide more accurate non-destructive techniques for forest biomass estimation. This research will contribute to the theoretical foundation and reference for forest resource surveys, ultimately enhancing the efficiency and precision of forest biomass estimation and contributing to more sustainable forest management practices.

2. Materials and Methods

2.1. Study Site

This study selected the Olympic Forest Park in Beijing as the research area. Located in the Chaoyang District, north of the Fifth Ring Road in Beijing, the Olympic Forest Park is situated at geographic coordinates 116°23′2.98″ E, 40°01′3.00″ N. The park spans an area of 680 hectares, predominantly featuring arbor and shrub vegetation, with a green area of 478 hectares, resulting in a high green coverage rate of 95.61%. The park's climate is characterized by a temperate continental monsoon climate with distinct seasons and concentrated precipitation. The average annual temperature is 11 °C, with an average annual precipitation of about 600 mm. Spring is dry and windy, with significant temperature differences between day and night; summer is hot and rainy; autumn is clear and less rainy, with comfortable temperatures and ample sunlight; winter is cold and dry, with windy conditions and a little snow.

The Olympic Forest Park boasts mature plantations characterized by detailed age classifications ranging from newly planted saplings to trees over 30 years old. The diverse flora includes over 100 species of trees, more than 80 species of shrubs, and over 100 varieties of ground cover plants. Predominant tree species include the Chinese white poplar (*Populus tomentosa*), Oriental arborvitae (*Thuja orientalis*), torch tree (*Paulownia tomentosa*), pine (*Pinus*), and ginkgo (*Ginkgo biloba*). Regular pruning, thinning, and controlled burns form a crucial part of the management practices, enhancing healthy growth and reducing disease incidence. The primary tree species, the Chinese white poplar, is a deciduous tree noted for its straight, towering trunk, rapid growth, lush foliage, deep roots, and excellent drought resistance. Its adaptability allows it to thrive in various soil conditions including clay, sandy loam, or slightly saline–alkaline soils. This versatility makes it extensively used in fast-growing timber plantations, protective forests, and in landscaping along roadsides and waterways.

2.2. Data Investigation

A plot of Chinese white poplar (*Populus tomentosa*) was meticulously chosen as the sample plot for this study. This square plot, measuring 40 m on each side, covers a total area of 1600 square meters. Positioned on a gentle slope, it exhibits distinctive ecological features. The plot is densely populated with 246 individual trees, creating a high canopy closure that significantly restricts sunlight penetration. This results in a sparse undergrowth and few shrubs beneath the dense canopy. The soil within the plot is primarily sandy loam, an ideal substrate for *Populus tomentosa* due to its adaptability to different soil conditions. Additionally, the layout of the plot facilitates easy navigation for surveyors and accommodates various measurement instruments and conditions, ensuring efficient data collection.

2.2.1. Ground Data

On 16 April 2022, manual data collection was conducted for the plot, employing a total station to ascertain the position of each tree, and a Differential Global Positioning System (DGPS) to determine the plot's corners and center point. The DGPS and laser radar data were coordinated using the same projection system, and it was necessary to align the total station data with the DGPS projection system [36].

Measurement parameters included tree height and diameter at breast height (DBH) for each specimen within the plot. Tree heights were measured with a laser height meter, while DBH values were obtained using a tape measure. Within the sample plot, the maximum tree height recorded was 24.08 m, and the maximum DBH was 78.70 cm. Conversely, the

minimum tree height was 9.87 m, and the minimum DBH was 14.57 cm. The average measurements indicated a tree height of 18.05 m and a DBH of 31.44 cm. Detailed results are presented in Figure 1.
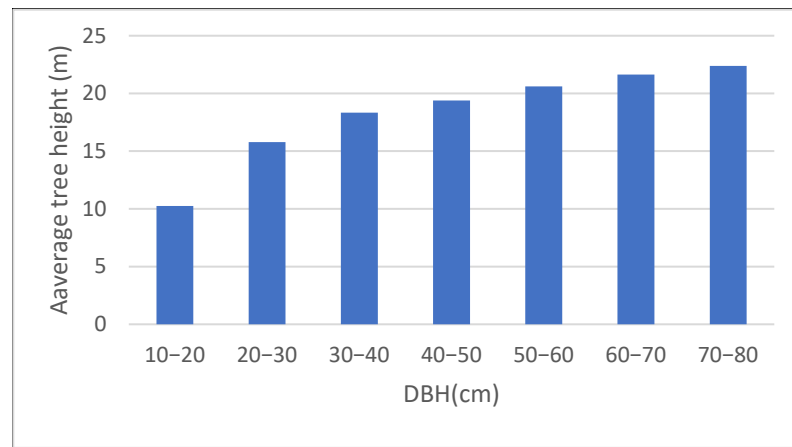

Figure 1. Measurements of tree height and DBH of tree.

2.2.2. Terrestrial Laser Scanning Data

On 13 April 2022, terrestrial laser scanning data were collected using a tripod setup. The FARO (Lake Mary, FL, USA) Laser Scanner Focus3D X330 was utilized for both single-station and multi-station scanning within the plot. The scanning data were imported into FARO SCENE 2020 software for point cloud stitching, resulting in the generation of three-dimensional point cloud data for the plot [37,38], as illustrated in Figure 2. Since the tripod-based TLS captures point clouds from beneath the canopy, it allows for clear identification of tree trunk information.

Figure 2. Point cloud data of terrestrial laser scanning.

2.2.3. Backpack Laser Scanning Data

On 14 April 2022, backpack laser scanning data were collected using the Libackpack50 (Berkeley, CA, USA) laser scanning system. This system combines laser scanning with simultaneous localization and mapping (SLAM) technology to acquire high-precision three-dimensional point cloud data of the plot in real time without the need for GPS (GNSS).

In this study, starting from the center of the plot, a figure-eight loop scanning pattern was implemented, which allowed for the capture of three-dimensional point cloud data of the plot with fewer noise points [17]. The data obtained, as shown in Figure 3, indicate that due to the flat terrain of the research plot and the stable walking of the surveyor with the BLS, there was minimal instrument shaking, resulting in more accurate tree point clouds. However, due to the height limitations of the BLS, the collection of canopy information was less effective.
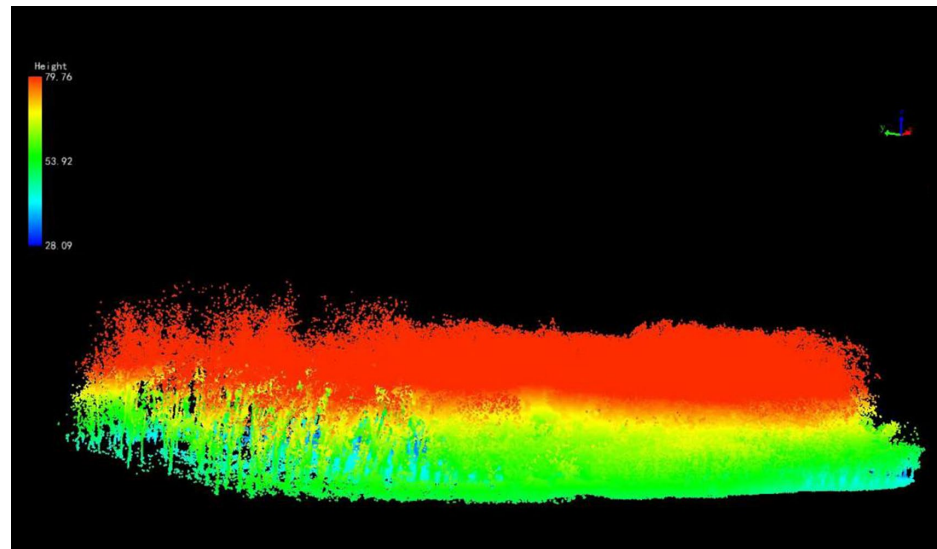
Figure 3. Point cloud data of backpack laser scanning.

2.2.4. Handheld Laser Scanning Data

On 15 April 2022, handheld laser scanning data collection was carried out. The ground-moving laser scanning was performed using the ZEB-REVO (Centurion, South Africa) handheld scanner, with a scanning platform height set at 1.5 m. The scanning was conducted in a closed Z″-shaped pattern, allowing for the acquisition of panoramic scanning point cloud data of the plot in a single walk. However, to ensure the completeness and accuracy of the data, areas within the plot were scanned multiple times along a path to ensure that each individual tree was thoroughly scanned [19]. The point cloud data obtained, as shown in Figure 4, indicate that due to the high canopy closure in the study area, there may be fewer scanning points in the canopy area.
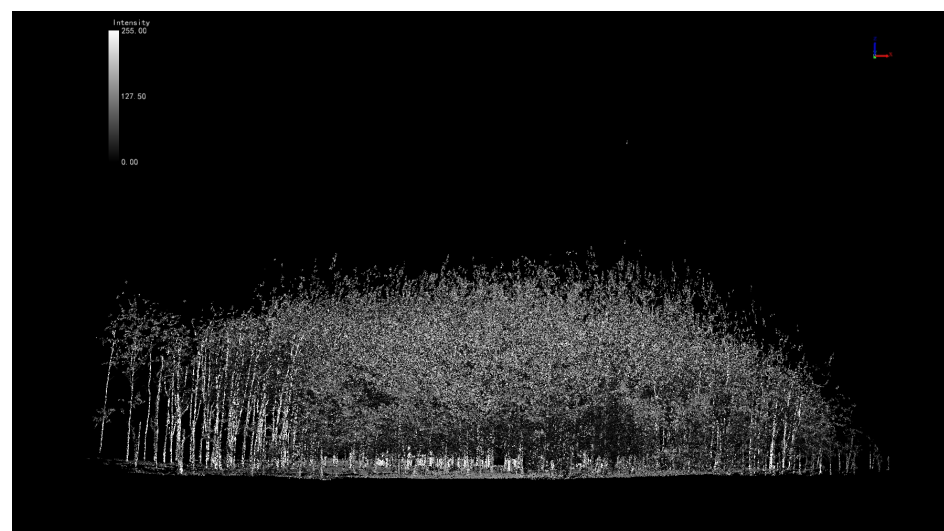
Figure 4. Point cloud data of handheld laser scanning.

2.3. Methodologies

2.3.1. Point Cloud Data Processing

The software used for point cloud data processing in this study is Lidar360 V7.0, a powerful platform for processing and analyzing LiDAR point cloud data. It features over 10 advanced point cloud data processing algorithms, capable of simultaneously computing and processing large-scale point cloud data exceeding 300 G. This software provides relevant applications for the terrain, forestry, and electric power industries.

Due to potential instrument errors, human operational inaccuracies, or external environmental factors, the point cloud data may include noise points unrelated to the scope of the experiment, such as environmental elements, ground objects, and non-ground points. These not only increase the quantity of point clouds, making processing more challenging but may also affect the precision of biomass estimation. The Lidar360 software employs an automatic denoising algorithm, which sets the number of neighboring points to 10 and the standard deviation multiplier to 5. It searches for adjacent points within a specified neighborhood for each point, calculates the average distance to neighboring points, and the median and standard deviation of these average distances. If the average distance between two points is greater than the maximum distance (Maximum distance = Median + Standard deviation × Standard deviation), then the point is considered noise and is removed. After denoising, a visual inspection of the results is necessary, and any unrecognized noise points must be manually deleted [26].

To separate ground points from non-ground points in the plot point cloud data, the software employs an improved progressive triangulated mesh filtering algorithm for ground point separation, setting the grid resolution to 0.1 m, the ground point thickness to 0.1 m, and the smoothing window size to 5. Initially, a sparse triangulated mesh is generated using seed points, followed by iterative processing to progressively densify the mesh, until all ground and non-ground points are completely separated [26]. After the separation, the ground points undergo Triangulated Irregular Network (TIN) interpolation to create a Digital Elevation Model (DEM), which is then normalized to obtain a consistent reference plane.

To achieve detailed modeling and biomass estimation from point cloud data, it is necessary to segment individual tree point clouds within the plot using an automatic point cloud segmentation method. Initially, seed points for individual trees are generated, followed by manual editing to add unrecognized seed points or remove superfluous ones. The segmentation of individual trees is then carried out from top to bottom, based on these seed points, with a clustering threshold set at 0.2 m to control the efficiency and precision of the segmentation. The ground point height is set at 0.3 m, allowing only point clouds above this height to participate in the individual tree segmentation to mitigate the effects of ground point cloud thickness or weeds on the segmentation results. Additionally, setting minimum tree height and diameter at breast height helps filter out shrubs and small trees within the plot. This process may lead to over-segmentation or under-segmentation, which is corrected through human–computer interaction by editing, clearing non-target point clouds near trees, and deleting or adding wrongly segmented point clouds. Moreover, individual trees with poor segmentation results or those that cannot be segmented are excluded. Ultimately, data for 53, 50, and 56 individual trees were obtained using the terrestrial, backpack, and handheld laser scanning methods, respectively.

2.3.2. Biomass Estimation Models

1. Allometric biomass model

Individual tree biomass can typically be calculated using allometric biomass models, which are empirical models established based on field survey data that relate vegetation structural parameters to biomass. In these models, tree height and diameter at breast height (DBH) are used as independent variables to establish a biomass model, with individual tree biomass as the dependent variable, allowing for the calculation of biomass for tree trunks, branches, and leaves, separately. Since the region and tree species significantly influence

the results of allometric biomass models, this study presents an allometric biomass model for *Populus tomentosa* in the Beijing area, as shown in Table 1. In this model, D represents tree DBH in cm, H represents tree height in m, W_S represents stem biomass in kg, W_B represents branch biomass in kg, W_L represents leaf biomass in kg, and W_T represents the total aboveground biomass in kg. The biomass of individual tree components calculated using the allometric biomass model will be used as a reference value to compare with the results obtained through the AdQSM 3D reconstruction model.

Table 1. Allometric biomass model in Beijing for *Populus tomentosa*.

Biomass	*Populus tomentosa*
W_S	$W_S = 0.0231 \, (D^2H)^{0.9258}$
W_B	$W_B = 0.00121 \, (D^2H)^{1.1337}$
W_L	$W_L = 0.00063 \, D^{1.1706}$
W_T	$W_T = W_S + W_B + W_L$

2.   AdQSM model

The Quantitative Structure Model (QSM) algorithm facilitates rapid modeling of individual tree point cloud data. It begins by generating corresponding cover sets for the point clouds on the surface of an individual tree. Based on the characteristics of these cover sets, it determines the local direction and geometric characteristics of tree trunks and branches. A series of cylinders with varying radii, lengths, and orientations are fitted to each segment using the least squares method to reconstruct parts of the individual tree's structure. This allows for the accurate calculation of volumes, lengths, and other attributes of branches and trunks from the reconstructed structural model. The QSM model is primarily characterized by the following seven parameters: d, r, n, d′, r′, n′, and l. d and d′ represent the minimum distance between the centers of two cover sets, r and r′ represent the radii used to generate the spherical cover sets, n and n′ represent the minimum threshold of points required to form the spheres, and l denotes the ratio of the length to the radius of the fitted cylinders.

AdQSM (Advanced Quantitative Structure Model) is a novel QSM method that can reconstruct the three-dimensional branch and trunk geometry of individual trees from ground-based LiDAR point clouds. This method quantitatively calculates numerous attributes of trunks and branches (as shown in Figure 5). Beyond directly extracting basic forest measurement factors such as diameter at breast height (DBH) and tree height, more importantly, through the three-dimensional geometric structure, it is possible to directly extract parameters such as the volume of trees (including trunks and branches). This provides a new theory and method for LiDAR point cloud modeling in disciplines such as dendrology, forest management, and ecological carbon stock monitoring. The tree volume extracted using AdQSM, combined with the basic wood density, can be used to calculate the individual tree's aboveground biomass, as shown in Equation (1).

$$W = V \times WD \tag{1}$$

where W represents the aboveground biomass of individual tree components, V represents the volume of individual parts of the tree model reconstructed by AdQSM, and WD represents the basic wood density.

This paper extracts from related literature that the basic wood density of *Populus tomentosa* in China is 0.452 g/cm^3 [39]. Furthermore, by employing the artificial *Populus tomentosa* binary log volume equation, as shown in Equation (2), the volume of the tree can be estimated, which in turn allows for the estimation of the biomass of individual parts of the tree. The biomass of an individual tree can be divided by different organs into the biomass of the trunk (including bark), branches, and leaves, with the sum of these components constituting the total biomass of the individual tree [40,41].

$$V = 0.00006D^{1.85363}H^{0.99633} \tag{2}$$

where V represents the total volume of the individual tree in cubic meters (m^3), D represents the diameter at breast height (DBH) of the individual tree in centimeters (cm), and H represents the height of the individual tree in meters (m).
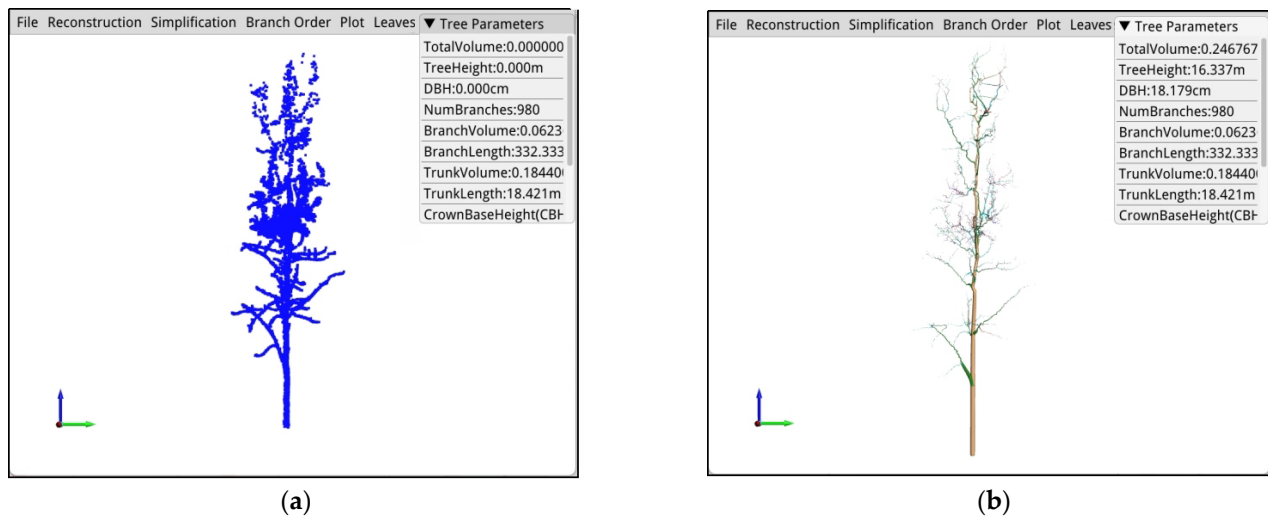

Figure 5. D reconstruction of the branch structure of single-wood (taking the point cloud data of handheld laser scanning as an example): (**a**) point cloud data; (**b**) model reconstruction.

3. Model Accuracy Evaluation

In this study, individual tree total biomass and the biomass of different parts (trunk, branches, leaves) were estimated based on terrestrial, backpack, and handheld laser scanning data using the allometric biomass model and the AdQSM model. The estimated values from the allometric biomass model were used as reference values to perform a linear regression analysis on the results of the AdQSM model. The fit of the two models was compared and analyzed using four indicators: (R^2), root mean square error (RMSE), relative root mean square error (rRMSE), and Pearson correlation coefficient (ρ), calculated using SPSS 26.0 software. The coefficient of determination R^2 represents the degree of model fit, RMSE and rRMSE represent the regression effect of the model, and the Pearson correlation coefficient ρ represents the similarity of model vectors. Larger values of R^2 and ρ indicate higher model fit and similarity, respectively, while smaller values of RMSE and rRMSE indicate better regression effect of the model. The calculation methods are shown in Equations (3)–(6).

$$R^2 = 1 - \frac{\sum_{i=1}^{n}(y_i - \hat{y}_i)^2}{\sum_{i=1}^{n}(y_i - \overline{y}_i)^2} \tag{3}$$

$$RMSE = \sqrt{\frac{\sum_{i=1}^{n}(y_i - \hat{y}_i)^2}{n}} \tag{4}$$

$$rRMSE = \frac{RMSE}{\overline{y}_i} \times 100\% \tag{5}$$

$$\rho = \frac{E[(X - \mu_X)(Y - \mu_Y)]}{\sigma_X \sigma_Y} \tag{6}$$

In the equation, y_i represents the reference value of the data, $\hat{y}_i$ represents the estimated value of the data, $\overline{y}_i$ represents the average value of the reference, n represents the number of samples, $X = X_1, \cdots X_n$ represents a reference vector of length n, and $Y = Y_1, \cdots Y_n$ represents an estimated vector of length n.

3. Results

3.1. Biomass Estimation Based on Terrestrial Laser Scanning Data

Based on the TLS point cloud data, the biomass of the trunk (W_S), branches (W_B), leaves (W_L), and the total aboveground biomass (W_T) estimated using the allometric biomass model (ABM) and the AdQSM model are presented in Table 2. The comparison of estimation results and the linear regression model is shown in Figure 6.

Table 2. Biomass estimation based on TLS.

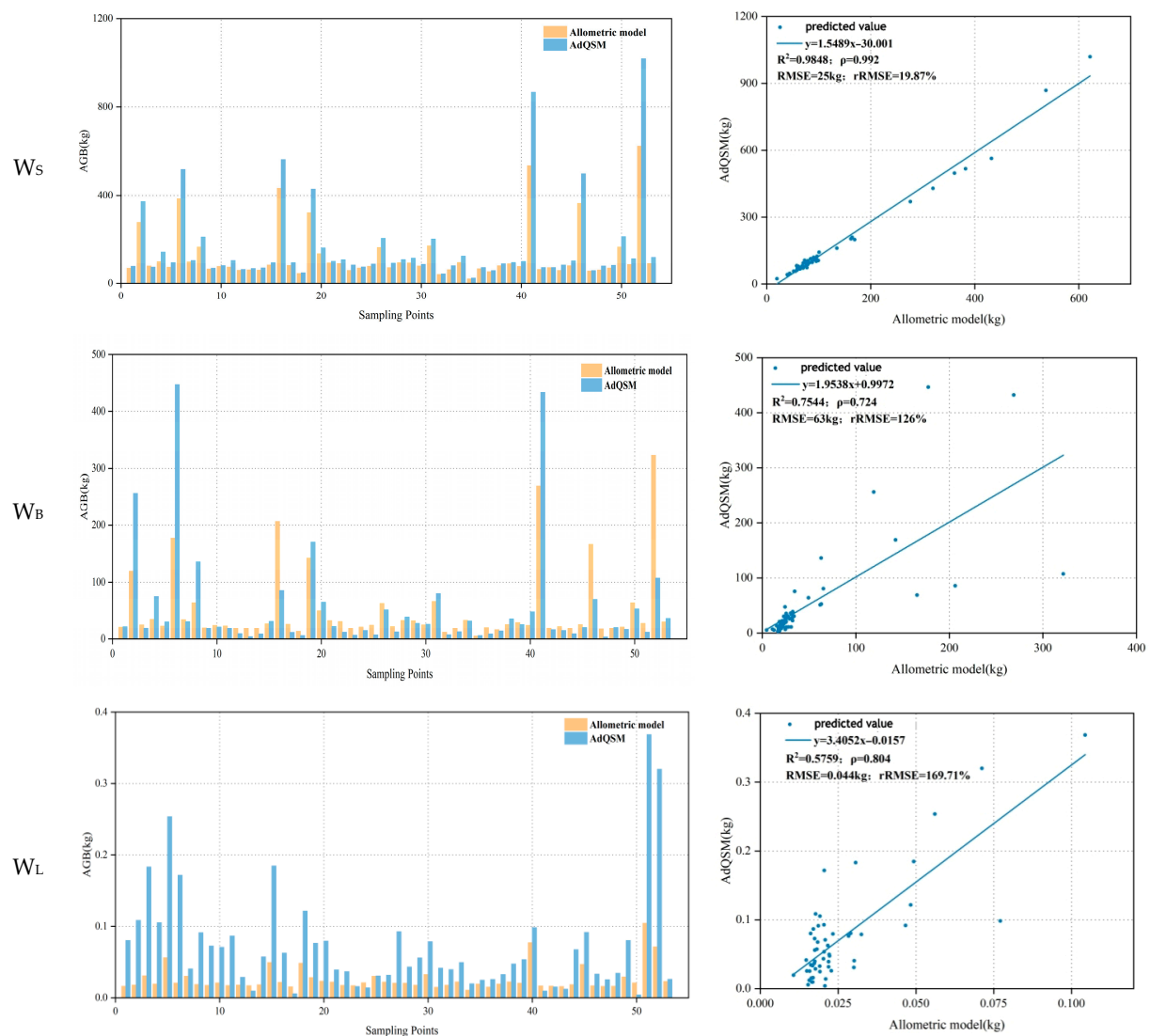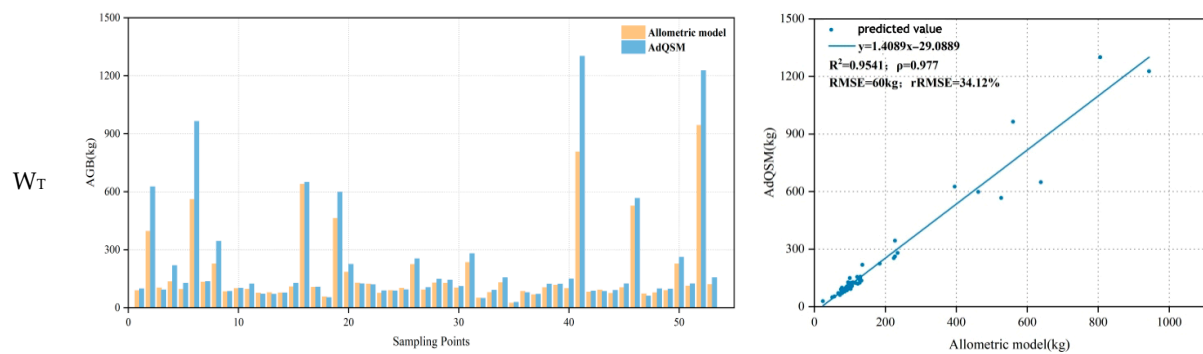| Result	Model	W_S/kg	W_B/kg	W_L/kg	W_T/kg
maximum value	ABM	621.7	671.9	0.1	943.5
	AdQSM	1019.1	684.7	0.4	1300.7
minimum value	ABM	19.7	4.7	0.0	24.4
	AdQSM	23.3	3.2	0.0	28.7
average value	ABM	125.8	61.5	0.0	175.8
	AdQSM	164.9	63.5	0.1	218.6

Figure 6. *Cont.*

Figure 6. The results of biomass estimation and the linear regression model based on TLS data.

From the graph, it can be observed that in terms of the coefficient of determination R^2, the order is W_S (R^2 = 0.9848) > W_T (R^2 = 0.9541) > W_B (R^2 = 0.7544) > W_L (R^2 = 0.5759), indicating that the estimation results of both models for individual tree trunk and total aboveground biomass have higher consistency, while the consistency of the estimation results for leaves is relatively lower. In terms of the relative root mean square error rRMSE, the order is W_S (rRMSE = 19.87%) < W_T (rRMSE = 34.12%) < W_B (rRMSE = 126%) < W_L (rRMSE = 169.71%), still indicating that the estimation results of both models for the trunk and total biomass have a smaller deviation. According to the Pearson correlation coefficient ρ, the order is W_S (ρ = 0.992) > W_T (ρ = 0.977) > W_L (ρ = 0.804) > W_B (ρ = 0.724), which also leads to the aforementioned results. From the comparison of result images, the red lines (using the AdQSM model) are mostly above the blue lines (using the allometric biomass model), suggesting that the estimation results using the AdQSM model are generally larger than those using the allometric biomass model, with a larger deviation in the estimated values of leaf biomass compared to trunk, branches, and total biomass. Looking at the linear regression equation, the coefficients of the linear terms (1.5489, 1.9538, 3.4052, 1.4089) are all greater than one, similarly indicating that the estimation results using the AdQSM model are overall larger than those using the allometric biomass model.

3.2. Biomass Estimation Based on Backpack Laser Scanning Data

Based on the BLS point cloud data, the biomass of the trunk (W_S), branches (W_B), leaves (W_L), and the total aboveground biomass (W_T) estimated using the allometric biomass model (ABM) and the AdQSM model are presented in Table 3. The comparison of estimation results and the linear regression model is shown in Figure 7.

Table 3. Biomass estimation based on BLS data.

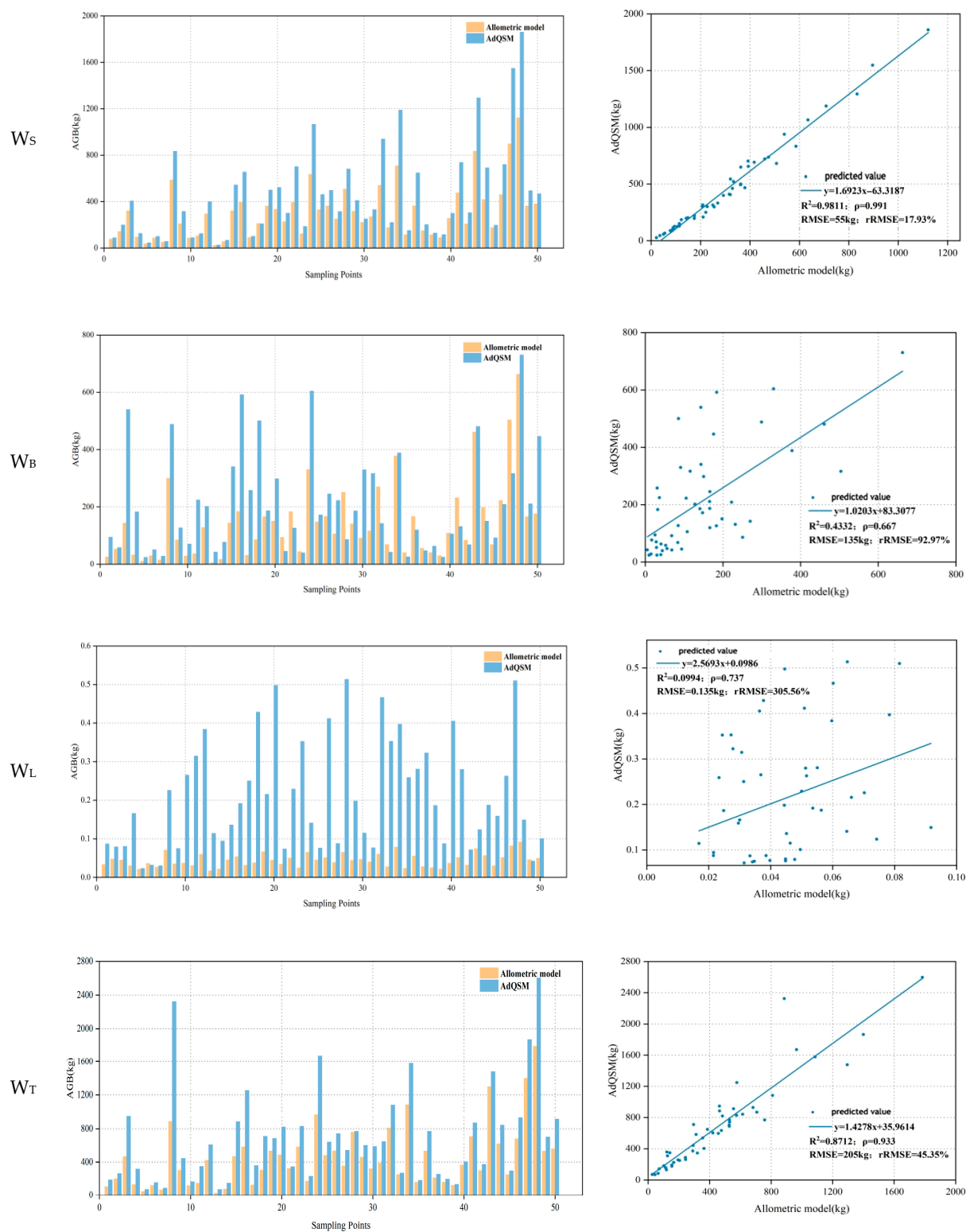| Result	Model	W_S/kg	W_B/kg	W_L/kg	W_T/kg
maximum value	ABM	1121.4	662.6	0.1	1784.1
	AdQSM	1859.8	730.2	0.5	2596.0
minimum value	ABM	21.8	5.3	0.0	27.2
	AdQSM	26.6	24.0	0.0	68.6
average value	ABM	306.8	145.2	0.0	452.0
	AdQSM	455.8	210.9	0.2	681.4

Figure 7. The results of biomass estimation and the linear regression model based on BLS data.

From the image, it can be observed that in terms of the coefficient of determination R^2, the order is W_S ($R^2 = 0.9811$) > W_T ($R^2 = 0.8712$) > W_B ($R^2 = 0.4332$) > W_L ($R^2 = 0.0994$). In terms of the relative root mean square error (rRMSE), the order is W_S (rRMSE = 17.93%) < W_T (rRMSE = 45.35%) < W_T (rRMSE = 92.97%) < W_L (rRMSE = 305.56%). According to the Pearson correlation coefficient ρ, the order is W_S ($\rho = 0.991$) > W_T ($\rho = 0.933$) > W_L ($\rho = 0.737$) > W_B ($\rho = 0.667$). From the comparison of the result images, the red lines (using

the AdQSM model) are mostly above the blue lines (using the allometric biomass model). Looking at the linear regression equation, the coefficients of the linear terms (1.6923, 1.0203, 2.5693, 1.4278) are all greater than one. This leads to consistent results with those estimated using the TLS: the estimation results of both models for individual tree trunks and total aboveground biomass have higher consistency, while the consistency of the estimation results for leaves is relatively lower; the estimation results using the AdQSM model are generally larger than those using the allometric biomass model, with a larger deviation in the estimated values of leaf biomass compared to trunk, branches, and total biomass.

3.3. Biomass Estimation Based on Handheld Laser Scanning Data

Based on the HLS point cloud data, the biomass of the trunk (W_S), branches (W_B), leaves (W_L), and the total aboveground biomass (W_T) estimated using the allometric biomass model (ABM) and the AdQSM model are presented in Table 4. The comparison of estimation results and the linear regression model is shown in Figure 8.

Table 4. Biomass estimation based on HLS data.

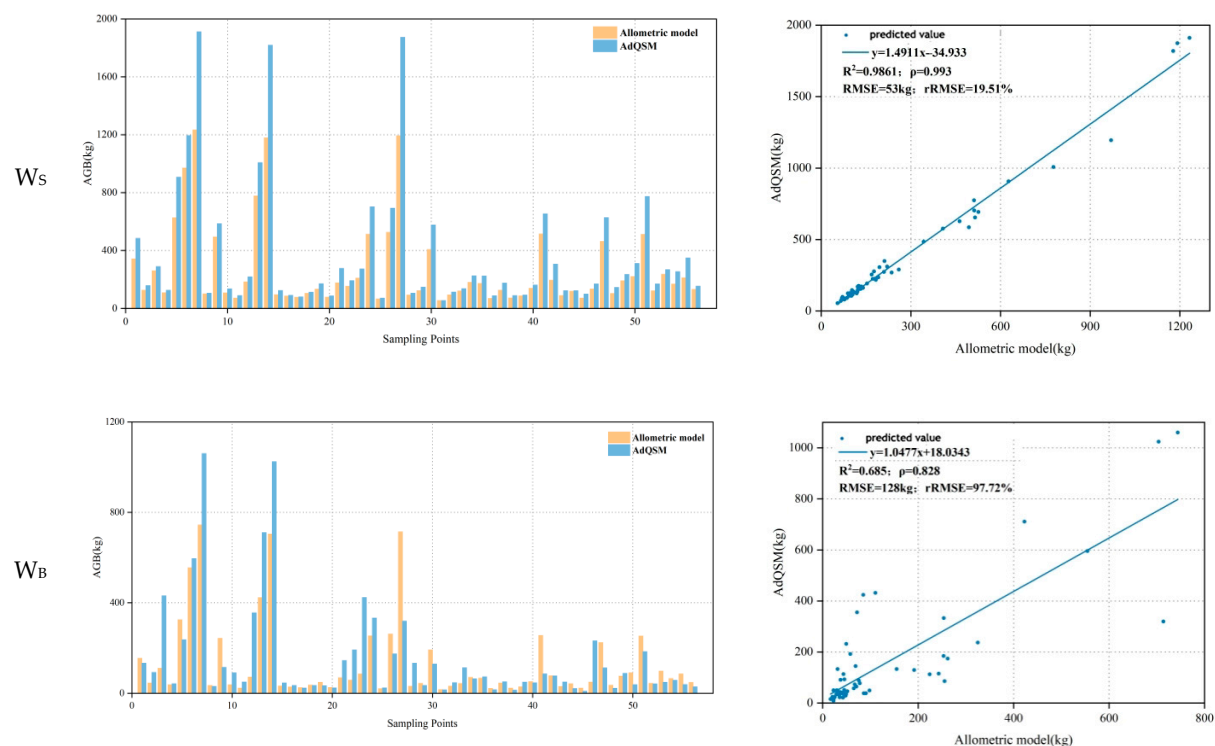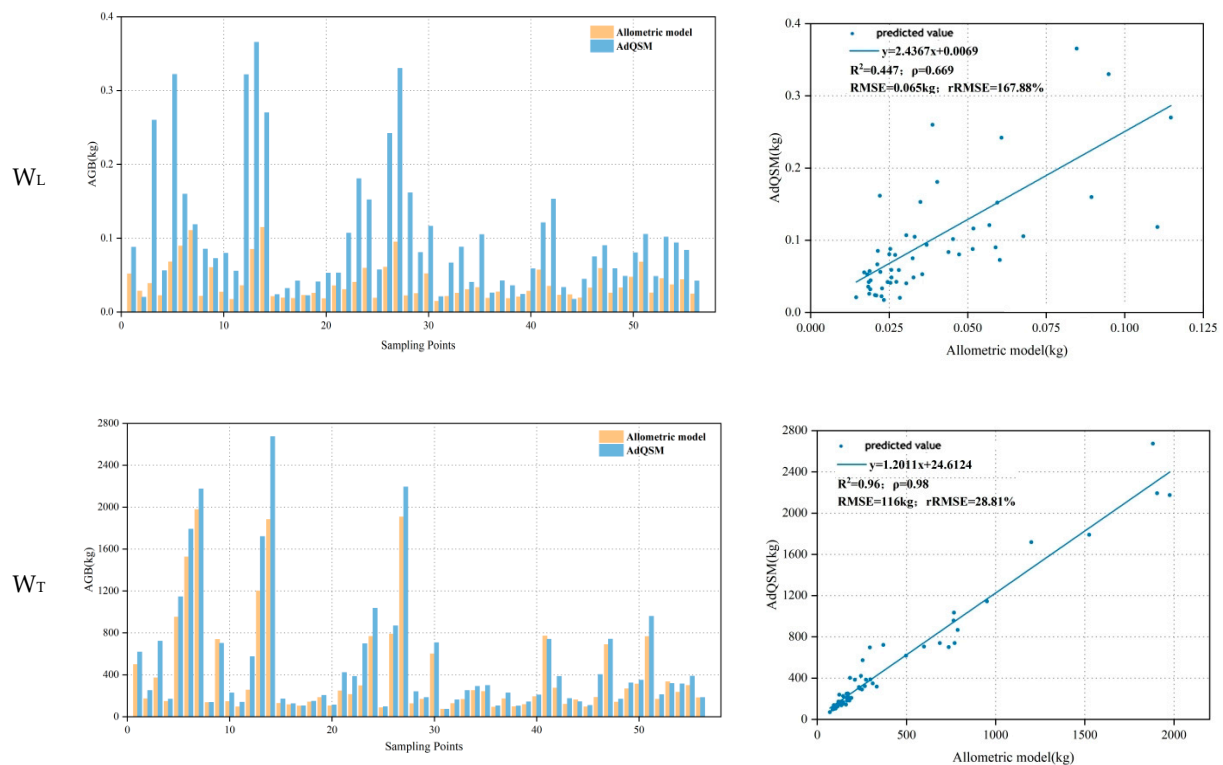| Result	Model	W_S/kg	W_B/kg	W_L/kg	W_T/kg
maximum value	ABM	1233.0	744.0	0.1	1976.8
	AdQSM	1910.9	1060.0	0.4	2673.2
minimum value	ABM	54.9	16.5	0.0	71.4
	AdQSM	54.9	9.0	0.0	70.2
average value	ABM	271.6	131.0	0.0	402.7
	AdQSM	370.1	155.3	0.1	508.2

Figure 8. *Cont.*

Figure 8. The results of biomass estimation and the linear regression model based on HLS data.

From the image, it can be observed that in terms of the coefficient of determination R^2, the order is W_S ($R^2 = 0.9861$) > W_T ($R^2 = 0.96$) > W_B ($R^2 = 0.685$) > W_L ($R^2 = 0.447$). In terms of the relative root mean square error (rRMSE), the order is W_S (rRMSE = 19.51%) < W_T (rRMSE = 28.81%) < W_B (rRMSE = 97.72%) < W_L (rRMSE = 167.88%). According to the Pearson correlation coefficient ρ, the order is W_S ($\rho = 0.993$) > W_T ($\rho = 0.98$) > W_B ($\rho = 0.828$) > W_L ($\rho = 0.669$). From the comparison of the result images, the red lines (using the AdQSM model) are mostly above the blue lines (using the allometric biomass model). Looking at the linear regression equation, the coefficients of the linear terms (1.4911, 1.0477, 2.4367, 1.2011) are all greater than one. This result is consistent with the biomass results estimated based on Terrestrial and Backpack Laser Scanning.

4. Discussion

In this study, the estimation of biomass for individual trees and various components using the AdQSM and traditional allometric models, based on three types of LiDAR point clouds, shows that the results of the two models are relatively close. However, QSM-based methods generally provide higher estimates than allometric equations. This difference is attributed to the QSM's detailed volumetric analysis, which may capture more structural complexities than the simpler allometric models. These findings align with existing research. Calders et al. [36] found that the biomass of individual trees estimated using the QSM model was 9.68% higher than the actual value obtained through destructive sampling, whereas the allometric growth equation estimated the biomass of individual trees to be between 29.85% and 36.57% lower than the actual value. Demol et al. [42] reported that the biomass of individual trees estimated using the QSM model was 0.75% lower than the actual value, and the biomass estimated using the allometric growth model was 7.8% lower than the actual value.

The estimation results for individual tree trunks and total aboveground biomass, based on the allometric biomass model and the AdQSM model, showed high congruence ($R^2 > 0.85$, $\rho > 0.9$, rRMSE < 50%). However, the estimation results for leaf biomass exhibited larger deviations ($R^2 < 0.6$), aligning with previous research findings. Dong et al. [43]

demonstrated that in the univariate additivity biomass model, the models for aboveground and trunk biomass had better fitting effects (R^2 > 0.9, RMSE < 0.2), whereas most models for belowground, branches, leaves, and canopy biomass had relatively smaller R^2 values and larger RMSEs. Additionally, the timing of this study's survey in mid-April, when the leaves of the artificial poplar forests in Beijing had not yet reached their full growth, also contributed to the lower leaf biomass results, with leaves accounting for less than 1% of the total aboveground biomass of individual trees.

Overall, the biomass estimation results based on the allometric biomass model and the AdQSM model are consistent, despite the AdQSM model typically providing higher estimates. In terms of technological improvements, this study utilized more detailed and higher precision LiDAR data to enhance the accuracy of biomass estimation, surpassing traditional methods that combine remote sensing with fieldwork, which are limited by image resolution and terrain accessibility [11,12]. We employed LiDAR technology to more effectively capture tree structure across various scales and distances. This technological advancement enables a more detailed and accurate depiction of tree architecture, which is essential for precise biomass calculations [14]. Building on this technology, we further compared biomass estimations using three distinct types of LiDAR point clouds: terrestrial, backpack, and handheld laser scanning data.

In terms of estimating the total aboveground biomass of individual trees, the deviations in the estimation values obtained using handheld (R^2 = 0.96, ρ = 0.98) and terrestrial (R^2 = 0.9541, ρ = 0.977) laser scanning data were smaller than those obtained using backpack laser scanning data (R^2 = 0.8712, ρ = 0.933), due to its performance limitation in extracting tree point clouds within a certain distance above the ground. Beyond this distance, the point clouds of backpack laser scanning become sparser, leading to poorer display results and inaccurate display of details, resulting in deviations in AdQSM modeling. This explains why studies on individual tree biomass estimation mainly utilize handheld and terrestrial laser scanning methods, with fewer employing the backpack laser scanning method.

This study provides more refined methodological references for non-destructive estimation of tree biomass, which is of significant importance for forest resource surveys and tree carbon sequestration calculations. However, this study also has some issues that need to be further researched in the future:

(1) Due to technical and research conditions, this study did not perform destructive sampling to accurately measure individual tree biomass; thus, the estimation accuracy of the allometric biomass model and AdQSM model could not be validated. In the future, if conditions allow, felling trees to accurately measure their biomass should be considered, to validate the accuracy of the aforementioned models.

(2) The study only targeted one location, Beijing, and one tree species, poplar. Future research should further diversify the study locations and tree species to verify the universality of the conclusions of this paper.

(3) Due to technical reasons, this study did not conduct biomass spatial mapping. In the future, if conditions permit, it could be combined with optical remote sensing image data to achieve spatial visualization of biomass.

5. Conclusions

This study primarily uses data from terrestrial, backpack, and handheld ground-based LiDAR point clouds at plot level to estimate the total biomass of individual trees and various biomass components, including trunk biomass, branch biomass, and leaf biomass. It employs the allometric biomass model and the quantitative structure model (AdQSM) for estimation, and linear regression analysis is conducted on the estimation results for comparison between the two models, yielding the following conclusions:

(1) Comparison and Application of the Two Models for Biomass Estimation

For the three types of point cloud data, the biomass estimation values obtained using the AdQSM model are generally larger than those obtained using the allometric biomass model, consistent with previous findings.

In estimating trunk and total biomass, the deviation between the estimation values obtained using the two models is small ($R^2 > 0.85$, $\rho > 0.9$, rRMSE < 50%), indicating that the estimation accuracy of these two models is not significantly different. This also explains why both models are widely used in related research on biomass estimation.

The biomass of individual tree leaves constitutes only a small part of the total biomass of individual trees (less than 1%), and existing literature on aboveground biomass estimation mainly focuses on trunks and branches. Therefore, for most trees, the biomass of leaves can be considered less important.

(2) Comparison and Application of Biomass Estimation Using Three Types of LiDAR Point Clouds

Based on TLS and HLS point clouds, the consistency of the estimation results for the total biomass of individual trees and various biomass components using the allometric biomass model and AdQSM model is strong. Hence, terrestrial and handheld laser scanning methods are widely applied in biomass estimation research.

Based on BLS point clouds, there are certain deviations in the biomass estimation results using the two models. However, backpack laser scanning is still suitable for sites with fewer understory shrubs and small trees. It allows for the rapid and accurate monitoring of tree diameter at breast height, which can then be used to estimate biomass.

Author Contributions: Conceptualization, J.W.; methodology, Y.Z. and S.X.; formal analysis, S.L., X.L. and Q.F.; investigation, S.L., X.L. and Q.F.; writing—original draft preparation, Y.Z. and S.X.; writing—review and editing, Y.Z., S.X., S.L., X.L., Q.F., N.X. and J.W.; visualization, Y.Z., S.X., S.L., X.L., Q.F., N.X. and J.W.; supervision, J.W.; funding acquisition, J.W. All authors have read and agreed to the published version of the manuscript.

Data Availability Statement: The data presented in this study are available on request from the corresponding author.

Conflicts of Interest: The authors declare no conflicts of interest.

References

1. Armson, D.; Stringer, P.; Ennos, A.R. The effect of tree shade and grass on surface and globe temperatures in an urban area. *Urban For. Urban Green.* **2012**, *11*, 245–255. [CrossRef]
2. Mu, X.; Liu, Q.; Pang, Y.; Hu, K.; Zhang, Q. Estimation of Forest Aboveground Carbon Storage Based on Airborne LiDAR. *J. Northeast. For. Univ.* **2016**, *11*, 52–56.
3. Yu, X.; Lu, S.; Jin, F.; Chen, L.; Rao, L.; Lu, G. Evaluation of Ecosystem Services Function Value of Forests in China. *Acta Ecol. Sin.* **2005**, *25*, 2096–2102.
4. Li, J.; Li, Z.; Yi, H. The Relationship Between Forests and Global Climate Change. *J. Northwest For. Univ.* **2010**, *4*, 28–33.
5. Zhang, Z. Research on Estimation of Subtropical Forest Structure Parameters and Stock Volume Distribution Using Airborne LiDAR. Master's Thesis, Nanjing Forestry University, Nanjing, China, 2018.
6. Price, B.; Gomez, A.; Mathys, L.; Gardi, O.; Schellenberger, A.; Ginzler, C.; Thürig, E. Tree biomass in the Swiss landscape: Nationwide modeling for improved accounting for forest and non-forest trees. *Environ. Monit. Assess.* **2017**, *189*, 106. [CrossRef] [PubMed]
7. Churkina, G. The role of urbanization in the global carbon cycle. *Front. Ecol. Evol.* **2016**, *3*, 144. [CrossRef]
8. Kükenbrink, D.; Gardi, O.; Morsdorf, F.; Thürig, E.; Schellenberger, A.; Mathys, L. Above-ground biomass references for urban trees from terrestrial laser scanning data. *Ann. Bot.* **2021**, *128*, 709–724. [CrossRef] [PubMed]

9. Davies, Z.G.; Edmondson, J.L.; Heinemeyer, A.; Leake, J.R.; Gaston, K.J. Mapping an urban ecosystem service: Quantifying above-ground carbon storage at a city-wide scale. *J. Appl. Ecol.* **2011**, *48*, 1125–1134. [CrossRef]
10. Disney, M.I.; Boni Vicari, M.; Burt, A.; Calders, K.; Lewis, S.L.; Raumonen, P.; Wilkes, P. Weighing trees with lasers advances, challenges, and opportunities. *Interface Focus* **2018**, *8*, 20170048. [CrossRef]
11. Arp, H.; Griesbach, J.; Burns, J. Mapping in tropical forests: A new approach using the laser APR. *Photogramm. Eng. Remote Sens.* **1982**, *48*, 91–100.
12. Nelson, R.; Krabill, W.; Maclean, G. Determining forest canopy characteristics using airborne laser data. *Remote Sens. Environ.* **1984**, *15*, 201–212. [CrossRef]
13. Nilsson, M.; Brandtberg, T.; Hagner, O.; Holmgren, J.; Persson, Å.; Steinvall, O.; Sterner, H.; Söderman, U.; Olsson, H. Laser scanning of forest resources. In Proceedings of the Scand-Laser Scientic Workshop on Airborne Laser Scanning of Forests, Umeå, Sweden, 3–4 September 2003; pp. 43–51.
14. Naesset, E.; Buerknes, K.O. Estimating tree heights and number of stems in young forest stands using airborne laser scanner data. *Remote Sens. Environ.* **2001**, *78*, 328–340. [CrossRef]
15. Anderson, J.; Martin, M.E.; Smith, M.L.; Dubayah, R.; Hofton, M.; Hyde, P.; Peterson, B.; Blair, J.; Knox, R. The use of waveform LiDAR to measure northern temperate mixed conifer and deciduous forest structure in New Hampshire. *Remote Sens. Environ.* **2006**, *105*, 248–261. [CrossRef]
16. Lin, S. Inversion of Forest Canopy Clustering Index Based on LiDAR. Master's Thesis, University of Electronic Science and Technology of China, Chengdu, China, 2019.
17. Cai, S. Extraction of Tree DBH Based on Ground-Based LiDAR and Backpack LiDAR. Master's Thesis, Northeast Forestry University, Harbin, China, 2021.
18. Li, N. Key Technology Research on Tree Parameter Estimation Based on Ground-Based LiDAR. Master's Thesis, East China University of Technology, Nanchang, China, 2022.
19. Fan, W.; Liu, H.; Xu, Y.; Lin, W. Comparison of Single Tree Structure Parameter Extraction Accuracy Between Ground-Based LiDAR and Handheld Mobile LiDAR. *J. Cent. South Univ. For. Technol.* **2020**, *40*, 63–74.
20. Bauwens, S.; Bartholomeus, H.; Calders, K.; Lejeune, P. Forest inventory with terrestrial LiDAR: A comparison of static and hand-held mobile laser scanning. *Forests* **2016**, *7*, 127. [CrossRef]
21. Zhang, X.; Zheng, Y.; Wen, K.; Wang, P.; Wu, F. Estimation of Single Tree Factors of Eucalyptus Using Integrated Airborne and Backpack LiDAR. *For. Res. Manag.* **2022**, *6*, 131–137.
22. Kukko, A.; Kaartinen, H.; Hyyppä, J.; Chen, Y. Multiplatform mobile laser scanning: Usability and performance. *Sensors* **2012**, *12*, 11712–11733. [CrossRef]
23. Bosse, M.; Zlot, R.; Flick, P. Zebedee: Design of a spring-mounted 3-d range sensor with application to mobile mapping. *IEEE Trans. Robot.* **2012**, *28*, 1104–1119. [CrossRef]
24. Yao, T.; Yang, X.; Zhao, F.; Wang, Z.; Zhang, Q.; Jupp, D.; Lovell, J.; Culvenor, D.; Newnham, G.; Ni-Meister, W.; et al. Measuring forest structure and biomass in New England forest stands using Echidna ground-based LiDAR. *Remote Sens. Environ.* **2011**, *115*, 2965–2974. [CrossRef]
25. Raumonen, P.; Kaasalainen, M.; Åkerblom, M.; Kaasalainen, S.; Kaartinen, H.; Vastaranta, M.; Holopainen, M.; Disney, M.; Lewis, P. Fast Automatic Precision Tree Models from Terrestrial Laser Scanner Data. *Remote Sens.* **2013**, *5*, 491–520. [CrossRef]
26. Zheng, Y. Study on Single Tree Biomass Inversion Based on Ground-Based LiDAR Assisted Effective Crown Information. Master's Thesis, Northeast Forestry University, Harbin, China, 2020.
27. Wang, C. Single Tree Structure Parameter Extraction and Biomass Estimation Combining UAV-LiDAR and HMLS Point Cloud Data. Master's Thesis, Northeast Forestry University, Harbin, China, 2022.
28. Fan, W. Study on Single Tree Parameter Extraction and Stem Biomass Estimation Using Handheld LiDAR. Master's Thesis, Northeast Forestry University, Harbin, China, 2021.
29. Soares, M.L.G.; Schaeffer-Novelli, Y. Above-ground biomass of mangrove species. I. Analysis of models. *Estuar. Coast. Shelf Sci.* **2005**, *65*, 1–18. [CrossRef]
30. Asrat, Z.; Eid, T.; Gobakken, T.; Negash, M. Aboveground tree biomass prediction options for the dry Afromontane forests in south-central Ethiopia. *For. Ecol. Manag.* **2020**, *473*, 118335. [CrossRef]
31. Bi, H.; Turner, J.; Lambert, M.J. Additive biomass equations for native eucalypt forest trees of temperate Australia. *Trees Struct. Funct.* **2004**, *18*, 467–479. [CrossRef]
32. Seidel, D.; Albert, K.; Ammer, C.; Fehrmann, L.; Kleinn, C. Using terrestrial laser scanning to support biomass estimation in densely stocked young tree plantations. *Int. J. Remote Sens.* **2013**, *34*, 8699–8709. [CrossRef]
33. Calders, K.; Newnham, G.; Burt, A.; Murphy, S.; Raumonen, P.; Herold, M.; Culvenor, D.; Avitabile, V.; Disney, M.; Armston, J.; et al. Nondestructive estimates of above-ground biomass using terrestrial laser scanning. *Methods Ecol. Evol.* **2015**, *6*, 198–208. [CrossRef]
34. Hackenberg, J.; Spiecker, H.; Calders, K.; Disney, M.; Raumonen, P. SimpleTree-An Efficient Open Source Tool to Build Tree Models from TLS Clouds. *Forests* **2015**, *6*, 4245–4294. [CrossRef]
35. Fan, G.; Nan, L.; Dong, Y.; Su, X.; Chen, F. AdQSM: A new method for estimating above-ground biomass from TLS point clouds. *Remote Sens.* **2020**, *12*, 3089. [CrossRef]

36. Wang, T.; Gong, J.; Zhang, L.; Yue, Y. Research on Methods of Extracting Tree Parameters Based on Airborne LiDAR Point Cloud Data. *Sci. Surv. Map.* **2010**, *35*, 47–49.
37. Zhu, R. Extraction of Tree Parameters Based on Ground-Based LiDAR and Close-Range Photogrammetry. Master's Thesis, Beijing Forestry University, Beijing, China, 2021.
38. Chen, S. Study on Single Tree Parameter Extraction and Biomass Estimation Using LiDAR. Master's Thesis, Beijing Forestry University, Beijing, China, 2020.
39. Zeng, W.S. Developing Tree Biomass Models for Eight Major Tree Species in China. In *Biomass Volume Estimation and Valorization for Energy*; IntechOpen: London, UK, 2017.
40. Meng, S.; Gu, Z.; Xiao, P.; Liu, Z.; Yu, J.; Peng, X.; Zhou, G. Characteristics and Model Research of Above-Ground Biomass Distribution of Pinus taeda in Ji'an Area of Jiangxi Province. *J. Beijing For. Univ.* **2022**, *44*, 41–51.
41. Chen, Z.; Cheng, G.; Bu, Y.; Huang, W.; Chen, J.; Li, W. Extraction of Single Tree Parameters of Broadleaf Forest Based on UAV Oblique Imaging. *For. Resour. Manag.* **2022**, *1*, 132–141.
42. Demol, M.; Verbeeck, H.; Gielen, B.; Armston, J.; Burt, A.; Disney, M.; Duncanson, L.; Hackenberg, J.; Kükenbrink, D.; Lau, A.; et al. Estimating forest above-ground biomass with terrestrial laser scanning: Current status and future directions. *Methods Ecol. Evol.* **2022**, *13*, 1628–1639. [CrossRef]
43. Dong, L.; Li, F. Biomass Estimation Models for Main Stand Types of Eastern Greater Khingan Mountains. *Chin. J. Appl. Ecol.* **2018**, *29*, 2825–2834.